Sensitivity of Established and Alternative Rear Occupant Thoracic Injury Metrics to Seat Belt Design Variables in Frontal Impacts

Marcy A. Edwards, Sushant R. Jagtap, Jessica S. Jermakian

Abstract Many studies have documented the thorax as the most likely body region for adults to sustain injuries in the rear seat in frontal crashes. This study explored options for accurately assessing the risk of thoracic injuries for rear-seat occupants in frontal test programmes by evaluating the sensitivity of various thoracic injury metrics to force limiting, pretensioning and belt position during loading. Nineteen sled tests were conducted using the HIII 5th female dummy while varying force limiting, pretensioning and shoulder belt position. Sternum deflection, thorax acceleration, electro-optical rib deflections and pressure mat thorax group loads all showed sensitivity to both force-limiting and pretensioning. Sternum deflection and electro-optical rib deflection, however, also showed a strong linear correlation with belt position. Sternum deflection for the standard belt and 3-kN load limiter and pretensioner belt, respectively, reported 2.7% and 2.3% reductions for every 5 mm of upward belt movement, which could have implications for crash test programmes when comparing the relative protection of restraint systems. The pressure sensor provided accurate dynamic belt positions. Thus, measurement of belt position with sternum deflection for the 5th female may provide testing organisations with information to interpret vehicle crash test sternum deflection results. The pressure sensor thorax group loads had strong correlations with sternum deflection when the belt position was constant, but showed little sensitivity to belt position indicating the sensor provides relevant information on load magnitude and distribution irrespective of belt position.

Keywords Advanced seat belt technology, frontal impacts, rear occupant thoracic injury, shoulder belt position, sternum deflection, thoracic injury metrics.

I. INTRODUCTION

Regulatory and consumer-information crash test programmes worldwide provide incentive for improvements in occupant protection in vehicle crashes. For frontal crashes, these programmes have historically prioritised reducing injuries for drivers due to higher occupancy rates. The gains made as a result of these programmes are reflected in Insurance Institute for Highway Safety (IIHS) crash test results, where the percentage of vehicles rated good in the IIHS moderate overlap crash test increased from 16% in 1995 to 100% by 2013 and are evident in field data where drivers of good-rated vehicles in the IIHS moderate overlap crash test are 46% less likely to die in a frontal crash than drivers of poor-rated vehicles [1]. Similarly, an analysis of U.S. New Car Assessment Program (U.S. NCAP) frontal test scores found correlation between composite scores and fatality rates for belted drivers in collisions from 1979-91 [2]. European New Car Assessment Programme (Euro NCAP) introduced occupant safety ratings for rear-seat occupants in frontal crashes in 2015, but U.S. crash test programmes conducted under Federal Motor Vehicle Safety Standards (FMVSS), the U.S. NCAP and the IIHS have yet to evaluate occupant safety for rear-seated occupants in frontal crashes. Consequently, advanced belt designs, like pretensioners and load limiters, and airbags that have improved safety for front-seat occupants [3], are less common in the rear seat. By 2008, all new U.S. cars were equipped with pretensioners and load limiters for the front-seat occupants [3]. But in 2020, less than 40% of the vehicles Consumer Reports rated had advanced belt designs in the rear seat, while in Europe advanced rear seat belt technology was equipped in almost all vehicles by 2020 [4]. Rear-seat safety has lagged front-seat safety to the point that the rear seat is now considered less safe than the front for certain age occupants, especially older adults [5].

To address this gap in protection, IIHS has been researching rear-occupant injuries and injury causation in frontal crashes. In 2019, reference [6] studied injuries in the National Automotive Sampling System-Crashworthiness Data System (NASS-CDS) and from police reports identified by the Fatality Analysis Reporting System (FARS), and documented thorax injuries as the most common injury for belted adults seated in the rear seat in frontal crashes. The specific thorax injuries observed included rib fractures, lung contusions,

M. A. Edwards (e-mail: medwards@iihs.org; tel: +1-434-985-4600) is a Senior Research Engineer, Sushant R. Jagtap is a Research Engineer and Jessica S. Jermakian is the Vice President of Vehicle Research at the Insurance Institute for Highway Safety in Ruckersville, Virginia, USA.

hemo/pneumothorax and heart or vessel damage, and it was found that these injuries predominately resulted from shoulder belt loading. This study confirms earlier findings from in [7] in 2005 that also documented the thorax as the most common location for injuries for rear-seated adult occupants and found that these injuries are most commonly due to belt loading.

The Hybrid III family of anthropomorphic test devices (ATDs), or dummies, have been the primary tools for assessing occupant injury in frontal crash tests for decades. To assess the risk of sustaining thorax injuries seen in field observations, these ATDs are equipped with a single rotary potentiometer that measures the deflection at the centre of the sternum and with thorax accelerometers mounted to the spine. Sternum deflection provides information about the loads sustained directly to the rib cage, which are the source of many life-threatening organ injures, whereas thorax acceleration represents the overall loads sustained by the thorax, including loading to more robust anatomical structures like the shoulder. The sternum deflection metric was developed and is calibrated to assess blunt loading to the centre of the thorax. Injury risk curves for sternum deflection have been developed for belt loading using belt load and injury data from field investigations in combination with ATD and PMHS sled testing, but these risk curves may not capture the risk of belt loading when not centred on the thorax [8,9]. Further, reference [10] studied the ability of the Hybrid III 50th male to predict real-world thoracic injury for restrained drivers and found that the vehicle metrics bumper-to-firewall distance and shoulder belt load were stronger predictors of real-world thoracic injury than sternum deflection. Reference [7] noted that while field data show thoracic injury as the most dominant for rear-seat occupants, crash test data dummy sensors indicate the head and neck have a higher likelihood of injury, and the researchers hypothesised that this discrepancy could be related to current injury threshold values or, since the Hybrid III dummy thorax biofidelity was optimized using hub impacts [8], a difference between the way ATDs and humans interact with the restraint systems. The THOR-50M ATD has been developed and a THOR-5F is under development to improve ATD thorax biofidelity and provide multi-axis and multi-point sensing for thorax deflection which may improve ATD predictions of human injury risk. However, the biofidelity of THOR's response to modern restraint designs has not yet been demonstrated. In a study of restraint optimization for the rear seat, reference [11] found that technologies such as 4-point belts or airbags produced greater THOR-50M chest deflections even as they reduced deflections measured with other ATDs. A recent study of driver injuries found that vehicles with higher THOR-50M deflections in crash tests had lower risk of serious thoracic injury in field crashes [12].

Other authors offer an additional contribution to the discrepancy between the HIII sternum deflection metric and real-world injury. Of the available frontals ATDs, the Hybrid III 5th female dummy best represents the average anthropometry of rear seated occupants who use the vehicle restraint system [13] yet, when reference [14] studied the effect of differing breast size and placement on the 5th female chest jacket before harmonisation they found that altering the belt path resulted in significant changes in sternum deflection. Reference [15] conducted a full-scale crash test paired comparison varying only belt position on the thorax of a Hybrid III 5th female and found that sternum deflections decreased by 18 mm with the belt positioned closer to the neck. Reference [16] also studied restraint design variables including seat pan design, belt position, load limiting and pretensioning with the HIII 5th female in the rear seat environment and reported decreases in sternum deflection values for high positions compared to lower positions with matched lateral axis positions. This is an important consideration for consumer-information testing since reference [17] in 2006 found a range of approximately 100 mm in belt position for both HIII 50th male and 5th female dummies, seated in the front seat across 98 NCAP tests. Range in belt position is likely to be even larger in the rear seat, where upper anchor locations vary significantly between vehicles.

Studies have reported the real-world benefits of belt technologies like force limiting and pretensioning in reducing thorax injuries [3,18]. Reference [19] reported an overall reduction in HIII ATD injury metrics without an increase in head excursion for the combination of dual-threshold force limiting plus pretensioning. Assessing the relative benefits of these technologies for rear-occupant thoracic injuries with accurate, meaningful metrics is an important next step for crash test programmes in addressing real-world occupant safety. The current study assesses and quantifies the sensitivity of current thoracic injury metrics (i.e., sternum deflection and thorax acceleration) and the additional metrics (i.e., electro-optical rib deflections and pressure sensor loads) to force limiting, pretensioning and belt position during loading.

II. METHODS

Nineteen tests were conducted on an acceleration sled with the seat oriented to simulate a frontal impact. Shoulder belt position on the thorax (measured vertically relative to the sternum potentiometer), pretensioning and force limiting were varied to study their effect on occupant kinematics and injury metrics, seat belt loads, and contact loads between the thorax and shoulder belt. Each of the three input parameters were investigated in isolation and then later in combination.

Shoulder belt position on the thorax was first investigated with a standard belt with no pretensioner or load limiter. The position of the belt on the thorax was varied by moving the shoulder belt, upper anchor location in the y-axis only (SAE J211 coordinate system) [20]. The shoulder belt position was varied from 11 mm to 81 mm above the sternum potentiometer ball location on the uncompressed thorax, for a total of six positions (11, 25, 39, 53, 67 and 81 mm), measured to the centre of the shoulder belt webbing in a dummy-based coordinate system. The shoulder belt positions used for data analysis were bounded on the low side by the lowest belt position, where the belt remained on the shoulder during the test (25 mm, Fig. 1a) and on the high side by contact with the moulded flesh at the neck (81 mm, Fig. 1b). For reference, the top center of rib 1 is located 78 mm above the sternum potentiometer ball and the bottom center of rib 6 is located 67 mm below the sternum potentiometer ball.

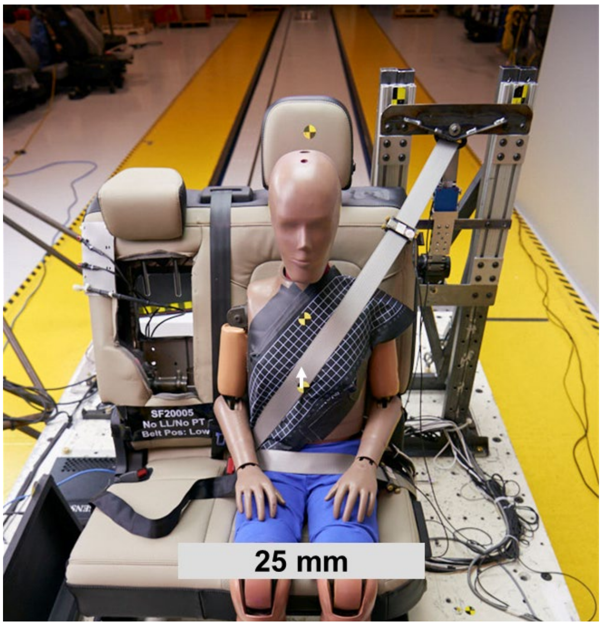

Fig. 1a. 25-mm belt position.

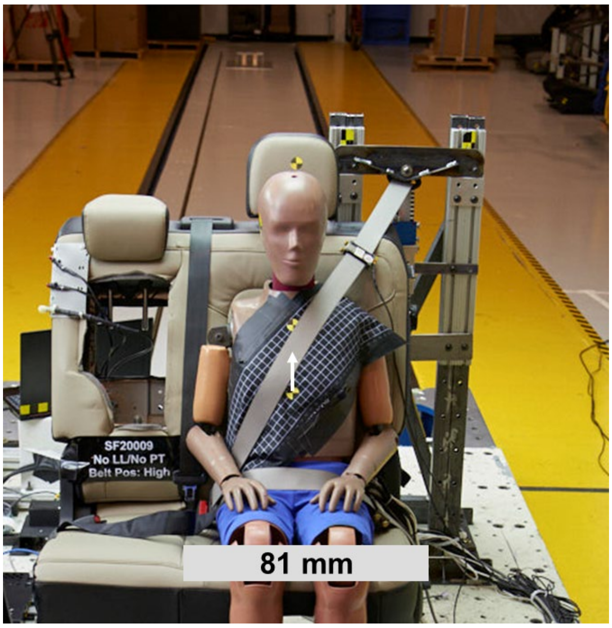

Fig. 1b. 81-mm belt position.

The effect of pretensioning was investigated with the belt positioned 25 mm above the sternum potentiometer and a load limiting threshold of 6.4 kN, which was chosen because pretensioner-only belts were not available, and it would not activate in these test conditions because of test severity and ATD mass. The pretensioner conditions investigated were no pretensioner, early deployed pretensioner and late deployed pretensioner. The early and late pretensioners were deployed so that belt movement began at 14 and 27 ms, respectively. Because of the time-zero offset on the sled, these times equate to 17 and 30 ms, respectively, in a vehicle. The labels “early” and “late” refer to their relative deployment timing in the event, but both times are within the range of pretensioner deployment times observed in vehicle tests. All seat belt assemblies were manufactured by Autoliv and all load limiters and pretensioners were located in the retractor.

Load limiting was investigated with the belt positioned 25 mm above the sternum potentiometer and no pretensioning. The standard belt with no load limiter was compared with belts with 3 kN, 4 kN, 5.5 kN, and dual-threshold (4.7/8.3 kN) load limiters.

After studying the parameters in isolation, their effects were then studied in combination. The effect of the load limiting threshold and pretensioning were further investigated by varying load limiting in combination with an early deployed pretensioner with the belt positioned 25 mm above the sternum potentiometer. The effect of belt position was further investigated in combination with a 3-kN load limiter and an early deployed pretensioner. See Table I for a complete description of all tests.

TABLE I
TEST MATRIX

Parameter	Force limiter	Pretensioner	Static belt position (above the sternum potentiometer)	Test ID
Low extreme	None	None	11 mm	SF20003
Baseline	None	None	25 mm	SF20005
Belt position	None	None	39 mm	SF20006
	None	None	53 mm	SF20007
	None	None	67 mm	SF20008
	None	None	81 mm	SF20009
Pretensioning	None*	Early	25 mm	SF20010b
	None*	Late	25 mm	SF20011
Force limiting	3 kN	None	25 mm	SF20014b
	4 kN	None	25 mm	SF20013
	5.5 kN	None	25 mm	SF20012
	Dual (4.5/7 kN)	None	25 mm	SF20015
Combined pretensioning and force limiting	3 kN	Early	25 mm	SF20016
	4 kN	Early	25 mm	SF20017
	5.5 kN	Early	25 mm	SF20018
	Dual (4.5/7 kN)	Early	25 mm	SF20019
Combined pretensioning, force limiting and belt position	3 kN	Early	39 mm	SF20020
	3 kN	Early	53 mm	SF20021
	3 kN	Early	67 mm	SF20022

*Force limiter thresholds were intentionally high so as not to activate in these tests.

The same acceleration pulse was used for all tests and was based on the average vehicle acceleration from 12 IIHS moderate overlap frontal crash tests at a 64.4-km/h impact speed with vehicles from varying classes (Fig. 2). The target delta V was 70 km/h, and the mean from all sled tests was 70.5 km/h with a standard deviation of 0.6 km/h.

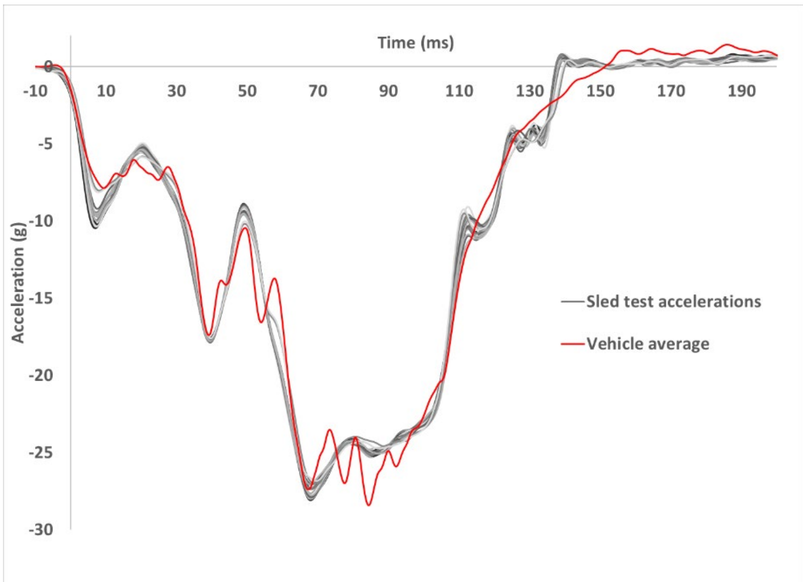

Fig. 2. Longitudinal acceleration target based on 12 moderate overlap crash tests and the sled test acceleration distribution.

The seat used was from the left second row of a 2020 Ford Escape 60/40 split bench seat. The seat pan was reinforced with urethane foam and thin aluminium plating to allow deformation but prevent cracking of the seat pan. The seat back was reinforced to prevent fatiguing of the recliner. The outboard lower anchorage location was replicated from the 2020 Ford Escape and the inboard buckle matched the original vehicle equipment. The upper anchor was positioned so that the belt did not interact with the seat back and the inboard/outboard location could be changed to vary the belt position on the thorax. The seat pan and anchor locations were inspected for damage after each test. Since little or no damage was found on the seat pan, the same seat pan was used throughout the test series. The entire seat belt assembly, including the buckle, was replaced for each test.

The IIHS *Dummy seating procedure for rear outboard positions, Version II Draft (October 2020)* was used to position a Hybrid III 5th female dummy (H35F) in the left seating position [21]. Subsequent tests matched the H-point, head centre of gravity and pelvic angle as closely as possible to the first test.

The dummy metrics included triaxial head accelerations and angular rates; thorax triaxial accelerations, y-axis angular rate and sternum potentiometer deflection; pelvis x- and z-axis accelerations and y-axis angular rate; upper neck, lower neck, thoracic spine, and lumbar spine x- and z-axis forces and y-axis moments; left and right iliac x-axis forces and y-axis moments; and femur axial forces. Instrumentation also included shoulder and outboard lap belt load cells and a belt spool-out sensor. All dummy and vehicle sensor data were collected at a sampling rate of 10,000 Hz in accordance with the SAEJ211 coordinate system [20]. To gather more information on deflection and loading related to thoracic belt loading, two additional sensors were included; the RibEye electro-optical system developed by Boxboro Systems [Boxborough, MA, USA], and Denton ATD, which can measure rib deflection on each of the 12 ribs and the XSensor high frequency, high-resolution pressure mat [Calgary, Canada], which provides contact locations and pressures between the shoulder belt and thorax.

The electro-optical deflection measurement system [RibEye, Boxboro Systems LLC, Boxborough, MA, USA] measures x and y locations for each of the 12 ribs using optical triangulation at a sampling rate of 10,000 Hz. Electro-optical sensors were placed on the ribs as shown in Fig. 3, ensuring that sensors were located to minimise error.

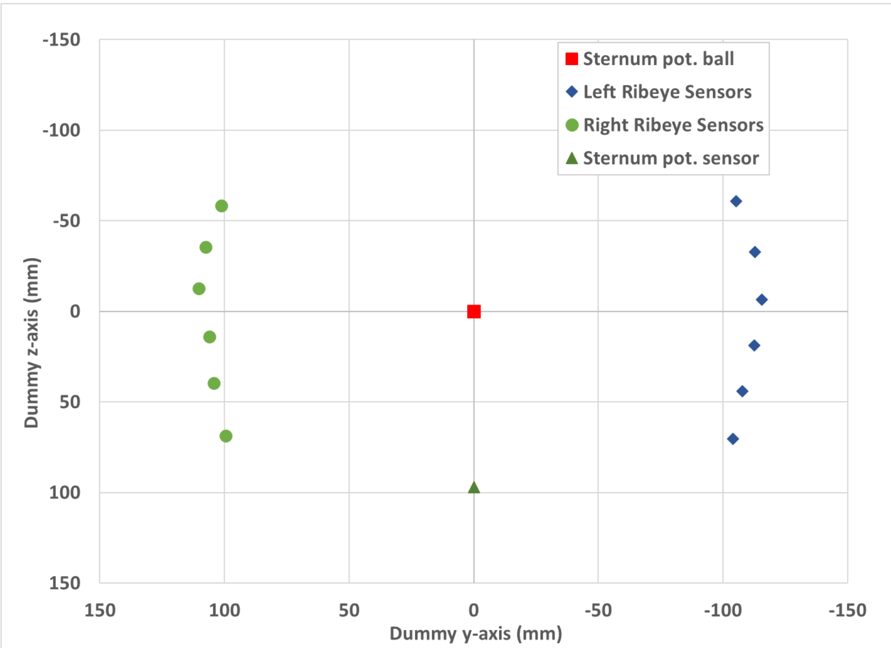

Fig. 3. Electro-optical rib sensor locations relative to the sternum potentiometer (anterior view of the interior portion of the anterior rib cage).

The pressure sensor mat [High Speed Impact System, XSensor, Calgary, Canada] provided time-dependent, two-dimensional mapping of the pressures between the seat belt and thorax at a frequency of 3900 Hz and a resolution of 5 x 15 mm. The location of the pressure mat was quantified relative to ATD landmarks with a 3D coordinate measurement machine (CMM) in a dummy-based coordinate system prior to the test, so that belt placement could be related to sternum potentiometer location. The pressure mat was secured to the ATD chest flesh using tape on all sides to prevent migration of the sensor relative to the flesh. In this sled series, film analysis confirmed that no belt migration was observed relative to the sensor grid so pretest-measured belt positions were used. However, since belt migration is often observed in vehicle testing, a methodology for establishing belt position at maximum sternum deflection was tested using the pressure mat. To locate the belt with the pressure sensor, the seat belt impression from the pressure-time data was used to identify the sensor rows and columns approximately along the centre of the belt. Sensor rows and columns were mapped prior to testing using a CMM, so row and column positions at the belt centerline could be mapped to y and z coordinates in the dummy-based coordinate system. Using the y and z coordinates for the belt centerline, a linear equation was made representing the local belt path. The belt path location relative to the sternum potentiometer was then calculated using the linear equation and sternum potentiometer coordinates (see Fig. 11).

To investigate the pressures reported by the pressure sensor, the pressure map results were divided into three groups (shoulder, thorax and shoulder and thorax combined) so that regions of interest could be targeted for analysis (Fig. 4). The thorax group included rows 15 to 25 on the pressure mat. The upper corner of thorax region aligned with the dummy clavicle holes which was used as a landmark to separate the shoulder region. The lower corner of thorax region aligned with the top of rib 6 and was selected to exclude any unrealistic localized loading due to folding of sensor in the lower right region. Aggregating the pressures over the total area of a group provided the measured load between the seat belt and the occupant. However, because of inaccuracies in calculating the loaded area and minimum pressure thresholds on the sensors, the loads calculated are an estimation. Additionally, there are cases where an isolated sensel value will exceed the calibration range in areas of high load concentration. Because these pressures are similar to the adjacent sensels that are within the calibration range, it not likely that this contributes large error to the results, but this is another contributor to the calculated loads being an estimation.

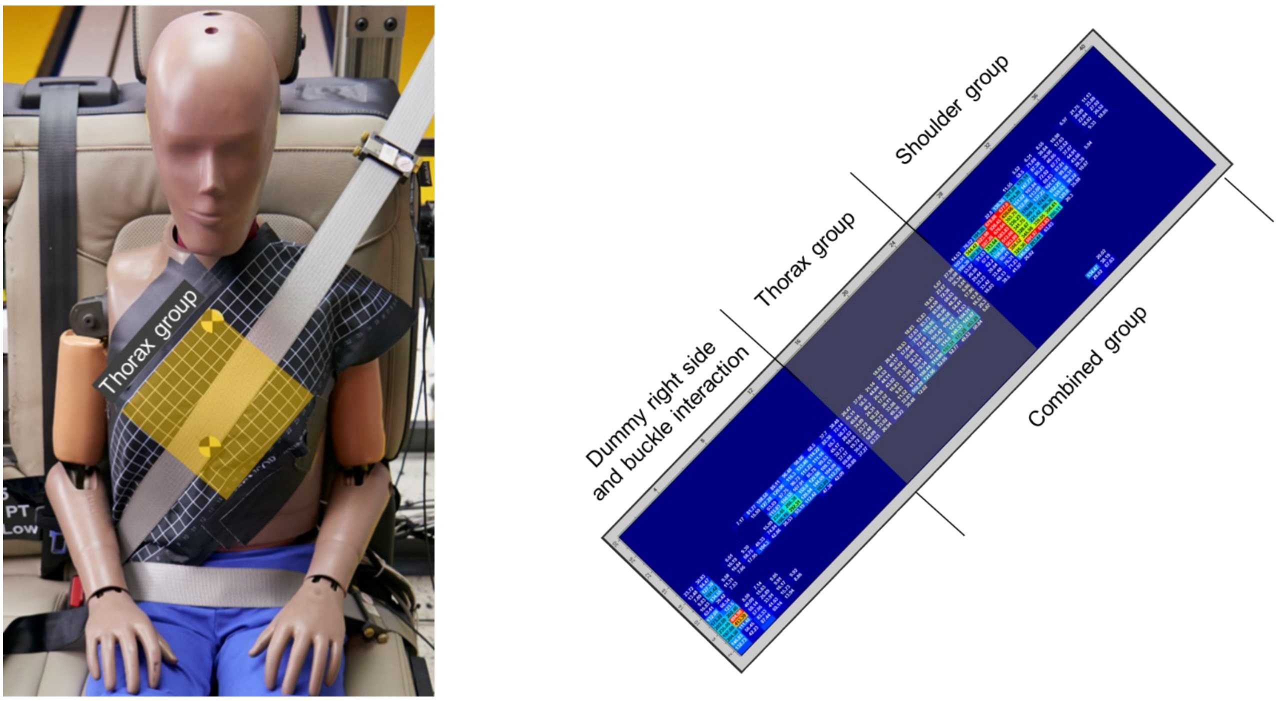

Fig. 4. Pressure mat group regions (captured at 90 ms) (sensor unit =psi)

III. RESULTS

The sensitivities of the sternum deflection, thorax acceleration, electro-optical rib deflections and pressure mat pressures measured on the Hybrid III 5th female dummy were studied with five load limiting conditions (none, 5.5 kN, dual with 4.5 and 7 kN, 4 kN and 3 kN), three pretensioner-deployment conditions (none, 14 ms and 27 ms) and five shoulder belt positions (25, 39, 53, 67 and 81 mm). Some of these variables were also studied in combination. Standard belts (without a pretensioner or force limiter) averaged 6.4 kN for shoulder belt load, and belts with force limiters and no pretensioners reported 5.5 kN (5.5 kN design), 5.0 kN (dual threshold with 4.5 and 7 kN design), 4.5 kN (4.0 kN design) and 3.0 kN (3.0 kN design), respectively. Shoulder belt loads not only reflected force limiting thresholds, but also showed reductions for the addition of a pretensioner. Table I provides a detailed list of parameters evaluated, and Appendix Table A-I includes test metric results.

Sternum Deflection (potentiometer)

Sternum deflection results show that the sternum deflection metric is sensitive to changes in force limiting and pretensioning. Fig. 5 shows that as force limiting threshold decreases, the resulting sternum deflection also decreases. The standard belt resulted in 48 mm of sternum deflection at the 25-mm position, but the addition of force limiting decreased the sternum deflection by 4 mm (5.5 kN), 7 mm (Dual 4.5/7 kN), 9 mm (4 kN) and 19 mm (3 kN), respectively, as the load limiter threshold decreased to a minimum sternum deflection of 29 mm for the 3 kN load limiter (no pretensioner) condition. Overall, at the 25 mm belt position, every 200 N increase in shoulder belt load resulted in a 1.1 mm increase in sternum deflection.

For the 3 kN load limiter condition, the addition of a pretensioner decreased the sternum deflection an additional millimeter to 28 mm. Most sternum deflections were reduced by the addition of an early deployed pretensioner, though some stayed almost the same. For the standard belt, deploying the pretensioner at 14 ms decreased sternum deflection by 2.6 mm, but deploying at 27 ms increased it by 1 mm.

Sternum deflection also showed sensitivity to shoulder belt position on the thorax. As the shoulder belt position moved higher, the sternum deflection linearly decreased. For the standard belt, Fig. 5 shows that raising the shoulder belt 56 mm (from 25 to 81 mm above the sternum potentiometer) decreases the sternum deflection by 15 mm, which is 37% of the sternum deflection injury assessment reference value (IARV) of 41 mm [22]. For belts that had advanced belt technology (3 kN load limiter and early pretensioner), raising the shoulder belt 42 mm decreased the sternum deflection by 5.4 mm, which is 13% of the IARV [22].

Fig. 5. also shows that raising the shoulder belt position on the thorax can result in sternum deflections equal to or lower than some belts with force limiting and pretensioning. For example, moving the shoulder belt up on the thorax by 14 mm (39 mm condition) with a standard belt gives a similar sternum deflection result as a belt with a 5.5 kN force limiter and pretensioner. Further, moving the shoulder belt up by 56 mm (81 mm condition) with the standard belt results in a sternum deflection even lower than seen with the 4 kN load limiter and pretensioner belt and moves the sternum deflection result across the IARV threshold.

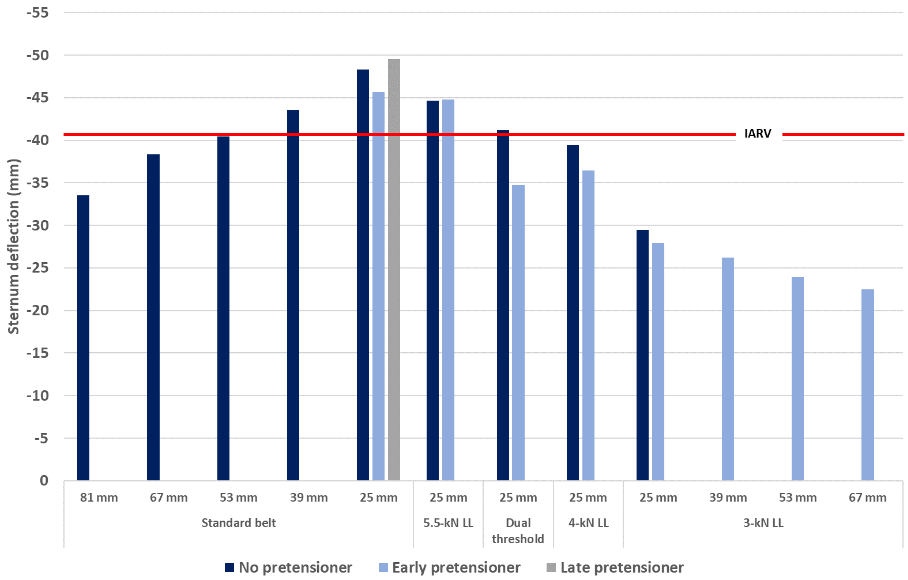

Fig. 5. Anterior-posterior sternum potentiometer deflection by belt position relative to chest potentiometer, pretensioner and load limiter (LL) characteristics.

Resultant Thorax Acceleration

Thorax acceleration also showed sensitivity to force limiting and pretensioning. Fig. 6 shows thorax acceleration decreasing with both force limiting threshold and with the addition of a pretensioner. Both the early and late pretensioner reduced thorax accelerations by approximately 5 g with the standard belt. Thorax accelerations showed little sensitivity to shoulder belt position. Moving the shoulder belt up by 56 mm (81 mm condition) with the standard belt increases the thorax accelerations 2 g, which is only 3% of the IARV of 73 g [22]. Moving the shoulder belt up by 42 mm (67 mm condition) with the 3 kN load limiter and pretensioner belt also increased the thorax accelerations by 2 g. Though these changes are small they do have an inverse relationship with the sternum deflection sensitivity, which may indicate that some of the decrease in sternum deflection can be attributed to an increase in thorax acceleration.

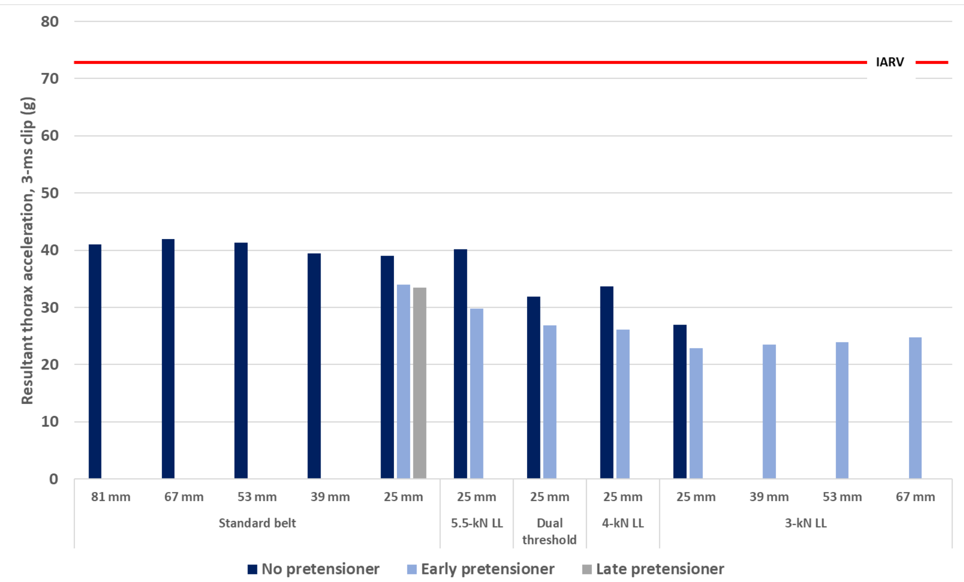

Fig. 6. Thorax resultant acceleration (3 ms clip) by belt position relative to chest potentiometer, pretensioner and load limiter (LL) characteristics.

Electro-optical Rib Deflection

Resultant rib deflections measured with the multi-point electro-optical system also showed sensitivity to force limiting and pretensioning and largely mimicked the trends of the sternum potentiometer. The maximum resultant deflection, which is the maximum resultant deflection reported by any rib, showed 52 mm of deflection with the standard belt at 25 mm, but the addition of force limiting decreased the maximum resultant deflection by 2 mm (5.5 kN), 6 mm (Dual 4.5/7 kN), 7 mm (4 kN) and 21 mm (3 kN), respectively, as the load limiter threshold decreased to a minimum of 31 mm of sternum deflection for the 3 kN load limiter (no pretensioner) condition (Fig. 7). The addition of a pretensioner further decreased the electro-optical maximum rib deflection by another 3 mm to 28 mm for the 3 kN load limiter condition. Also like sternum deflection, maximum resultant electro-optical rib deflection showed sensitivity to belt position. Ratios of maximum resultant rib deflection to sternum deflection remained constant at 1.1 across all standard belt positions, indicating that the maximum resultant deflection shows a sensitivity to belt placement similar to sternum deflection. Raising the shoulder belt above the thorax potentiometer from 25 to 81 mm decreased the maximum resultant rib deflection by 15 mm, the same amount as the sternum potentiometer. With the 3 kN load limiter and pretensioner belt, raising the belt from 25 to 67 mm decreased the maximum resultant deflection by 6 mm. However, some of these results were likely influenced by data loss for individual ribs with the electro-optical system. Losing data on the lower ribs (5 and 6) was a common issue in this dataset because of interference from the sternum potentiometer arm, and some reported maximum resultant deflections were taken from the remaining ribs reporting data. Based on deflection patterns in adjacent ribs, Fig. 7 indicates the maximum resultant rib deflections that would likely have been reported from the lost ribs if data loss had not occurred. In these cases, the reported maximum resultant rib deflections are likely lower than if data loss had not occurred. Appendix Table A-III shows a complete chart of individual rib resultant results and where data was lost.

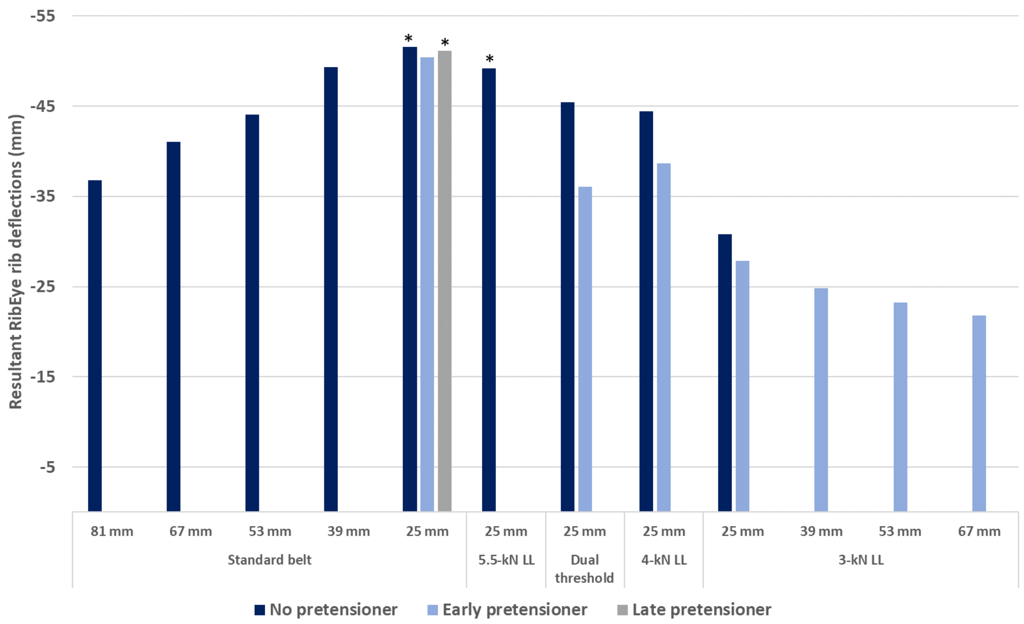

Fig. 7. Electro-optical resultant maximum deflections by belt position relative to chest potentiometer, pretensioner and load limiter (LL) characteristics. * Data loss on rib most likely to have reported electro-optical maximum deflection. Reported value is from the remaining ribs and is likely lower than if data loss had not occurred.

Comparison of electro-optical resultant rib deflections provides insight on load distributions. Fig. 8 shows the electro-optical rib deflections for each rib for all belt positions with the standard belt. The chart shows that that the primary loading for an occupant with a left shoulder upper anchor occurs on the right side of the thorax. Deflections on the right side of the thorax are consistently higher for all ribs. Figures 10 a and b show the belt path at the two belt position extremes and an estimation of the location of the top of rib 1. For both belt positions, most of the belt on the left side passes over the shoulder region and the gap between the ribs and shoulder. As the belt approaches rib 1 the belt is almost at the centerline of the dummy. This is more pronounced at higher belt positions. Due to occupant kinematics and anchor locations, the rigid shoulder bears most of the load on the left side of the dummy, reducing left side rib deflections. As the belt passes to the right side of the dummy, only the ribs interact with the belt, so the ribs bear almost all of the load on the right side of the dummy as the belt wraps around rib 6 to the latch plate.

Fig. 8 also shows that the rib reporting the maximum resultant deflection changed with belt position, but the maximum resultant deflection it reported decreased as the belt moved higher on the thorax. Between 25 and 39 mm, the ribs reporting maximum deflection were affected by data loss, but the slopes indicate that the maximum reporting rib (right rib 6) would not have changed. At the lower belt positions, the belt path is concentrated across the lower right ribs, which is reflected in the higher deflections for these ribs. However, as the belt continues to move upward, the deflections reported by the right ribs converge at the 67-mm position, which reflects the even distribution of the belt across the right ribs. At the highest position, 81 mm, the rib deflections diverge again but right rib 2 reports the maximum and right rib 6 reports the minimum. Though some data was lost for Fig. 8, the steeper slopes shown by the lower ribs (5 and 6) indicate that these are the most sensitive ribs to changes in belt position. Right Rib 1 shows 8 mm of change in deflection when moving the belt from 39 to 81 mm, while right rib 6 shows a 15 mm change in deflection for the same change in position. The sensitivity (or slope) of the sternum potentiometer, which Fig. 3 shows is located between ribs 3 and 4, aligns most closely with right rib 4.

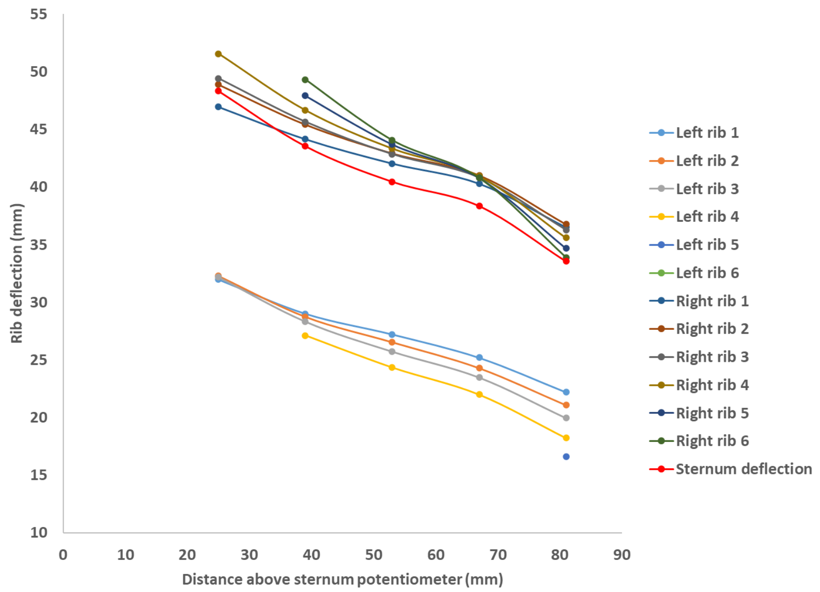

Fig. 8. Electro-optical rib resultant individual rib deflections by belt position for the standard belt.

Though differences were observed in the sensitivity of individual ribs to belt position, Fig. 9 shows less difference in the sensitivity of individual ribs to changes in force limiting at the 25 mm position. Ribs on the left side show more similarity in slope between ribs, indicating similarity in these ribs to sensitivity force limiting. Ribs on the right side show greater sensitivity to changes in shoulder belt load and slightly larger differences in sensitivity between the ribs.

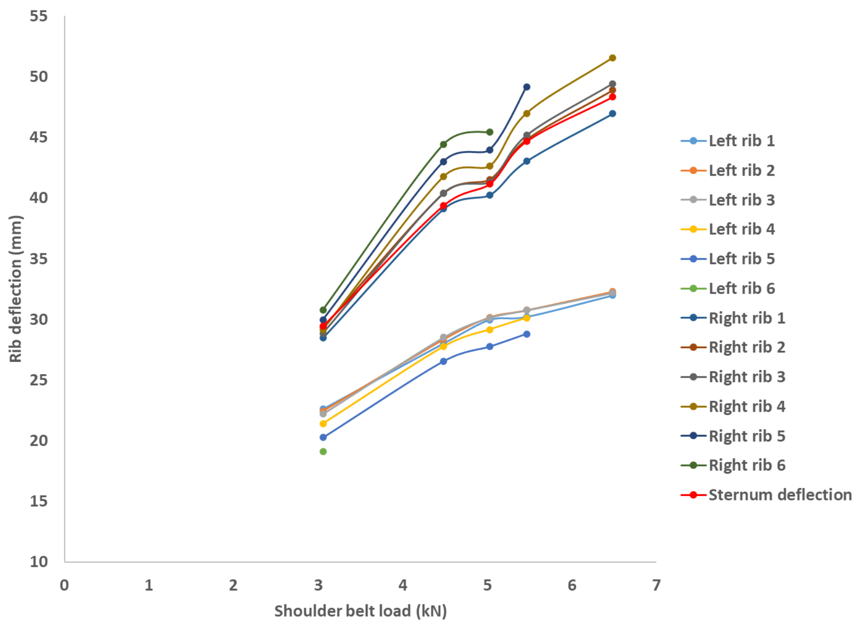

Fig. 9. Electro-optical rib resultant individual rib deflections by shoulder belt load for the 25-mm belt position.

Video analysis provides further insight into load distributions and the effect of belt position on sternum deflections. Figure 10 shows a comparison of belt loading with the belt positioned at 25 and 81 mm. When the belt is positioned at 25 mm, the belt path is centred on the thorax, which results in increased deflection of the ribs for this condition, especially the lower right ribs. In contrast, the belt positioned at 81 mm primarily loads the right side of the torso, where the curvature of the ribs translates the load to the spine, resulting in a 5-degree reduction in torso rotation about the y-axis and slightly higher thorax acceleration instead of rib deflection. The electro-optical system provides both anterior-posterior (A-P or X) and lateral-medial (L-M or Y) deflections which are provided in Table A-IV, which could also provide further insight into load distributions and occupant dynamics. Analysis of the A-P and L-M deflections individually show that deflections in both axes have similar trends to the resultant. As belt position moves higher both the A-P and L-M deflections decrease in magnitude.

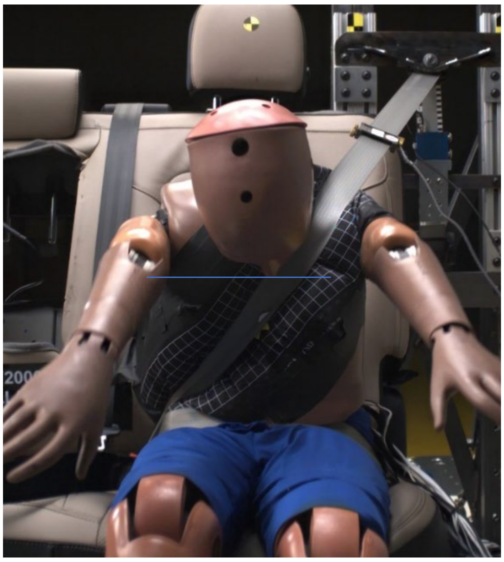

Fig. 10a. Belt loading at the 25-mm belt position. Estimated top of rib 1 shown in blue.

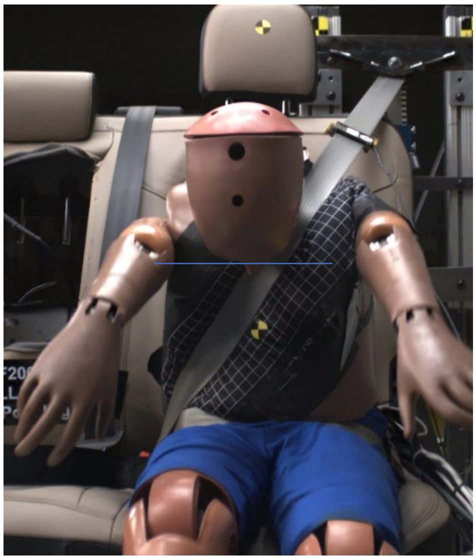

Fig. 10b. Belt loading at the 81-mm belt position. Estimated top of rib 1 shown in blue.

High Frequency Pressure Sensor

The high frequency pressure mat provided data for both the dynamic position of the shoulder belt and the distribution and magnitude of belt loading on the thorax. The dynamic position of the shoulder belt was measured by recording the location of the sensor and relevant dummy landmarks with a CMM in a dummy-based coordinate system prior to the test and then using the location of the belt pressure on the sensor to locate the belt path in the same coordinate system. In these sled tests, pretensioning did not affect belt position, so calculated belt locations at the onset of loading were compared with the pretest locations to check the accuracy of the methods. Fig. 11. below shows the pretest belt path compared with the belt path calculated using the centre of pressure of the seat belt on the pressure sensor. This comparison shows that the pressure mat calculated belt path is a good representation of the actual belt path. In this sample test, belt path was measured pretest at 25 mm above the sternum potentiometer and the pressure mat belt path was calculated at 27 mm.

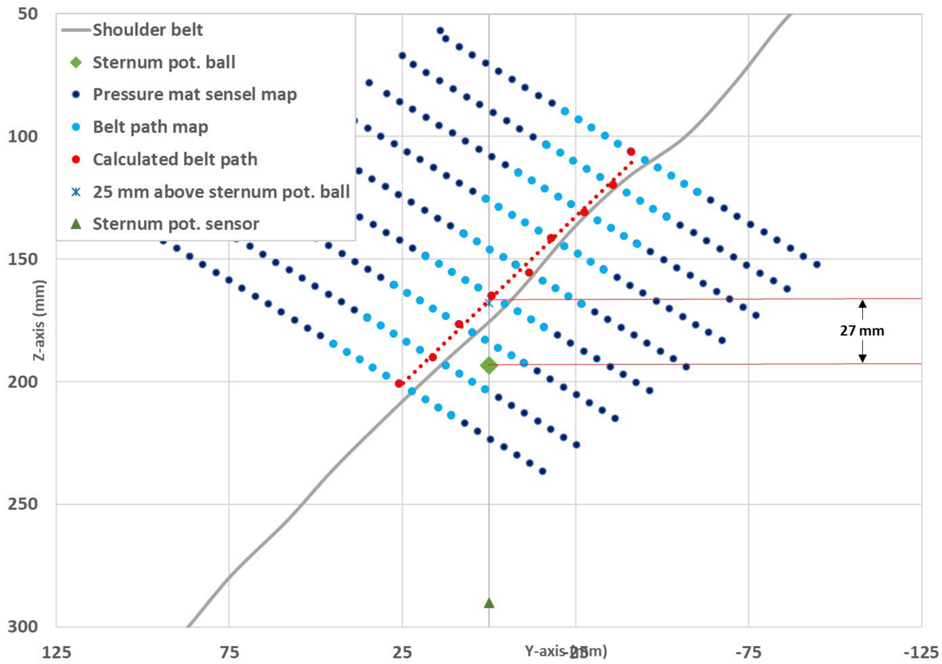

Fig. 11. Methodology for using the pressure mat to locate the dynamic belt position. Pressure mat sensel positions are for rows 16–25 in the dummy coordinate system.

The pressure mat also provided information on load magnitude and distributions. Post-processing of the load sensor allows the user to group the data into meaningful regions or *groups*. Data from the lower portion of the sensor that wraps around the side of the dummy and interacts with the buckle was eliminated due to sensor bunching and loading from the pelvis and lap belt. The remaining area was divided into the thorax region and shoulder region. To understand the relevance of particular regions and the estimated loads reported by them, results were evaluated for their correlation to sternum deflection, currently the best available indicator of thoracic injury using the HIII dummy, while varying force limiting and pretensioning, but keeping belt position constant. Three regions were assessed as shown in Fig. 4: the shoulder region, the thorax region and the two regions combined. Fig. 12. shows the estimated loads for each region and their correlation with sternum deflection for all tests where the belt position remained constant. The thorax region shows a strong correlation with sternum deflection (R^2 = 0.88), while the shoulder region does not. The combined region is strongly influenced by the shoulder region and also does not show correlation with sternum deflection.

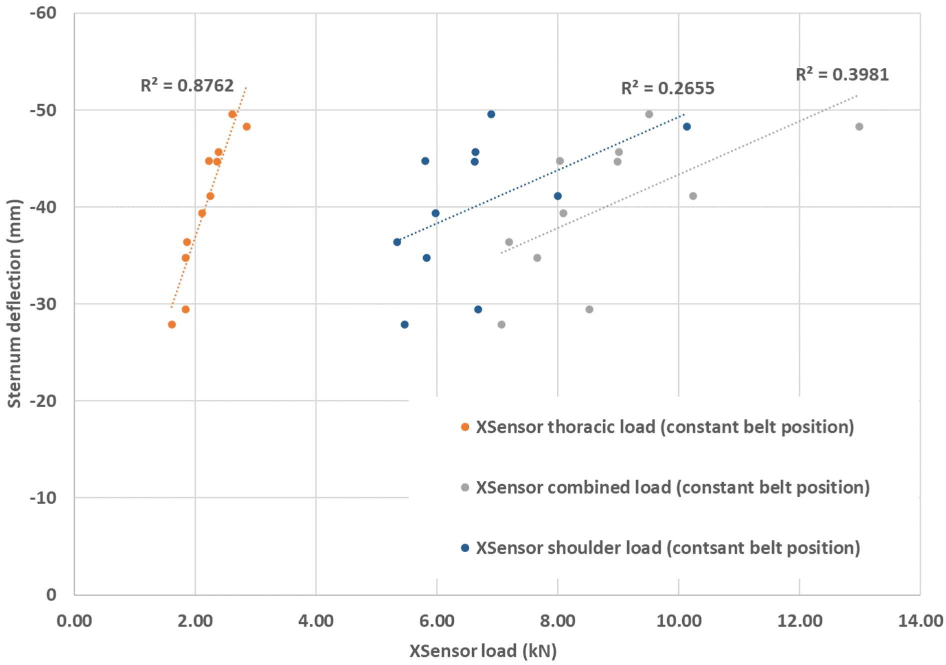

Fig. 12. Correlation of pressure mat thorax, shoulder and combined group loads to sternum deflection for all tests where force limiting and pretensioning varied but belt position remained constant (tests at the 25 mm position in Fig. 8 and 9).

The shoulder and thorax region estimated loads were further investigated for sensitivity to force limiting, pretensioning and belt position. Fig. 13 shows that the thorax region estimated loads do show sensitivity to both force limiting and pretensioning, but little sensitivity to belt position. Between the standard belt and 3 kN load limiter belt, thorax loads decreased linearly by 36%, from 2.85 kN to 1.83 kN. Pretensioning reduced the thorax loads by 17% with the early pretensioner for the standard belt; like sternum deflection, loads with the late pretensioner were higher than the early pretensioner. Thorax loads at the 25 mm belt position showed some variance with belt position, but the rest did not. In Fig. 14, shoulder group loads decreased by 35% with the addition of a 5.5 kN load limiter, however, further decreases in load limiting threshold did not further reduce shoulder loads. Pretensioning also had a significant impact on shoulder loads with the standard belt, reducing loads 34%. Pretensioning also lowered shoulder loads for force limited belts, but to a lesser degree averaging only 17% reductions. Shoulder group loads show some variance with belt position, but not a consistent sensitivity to belt position.

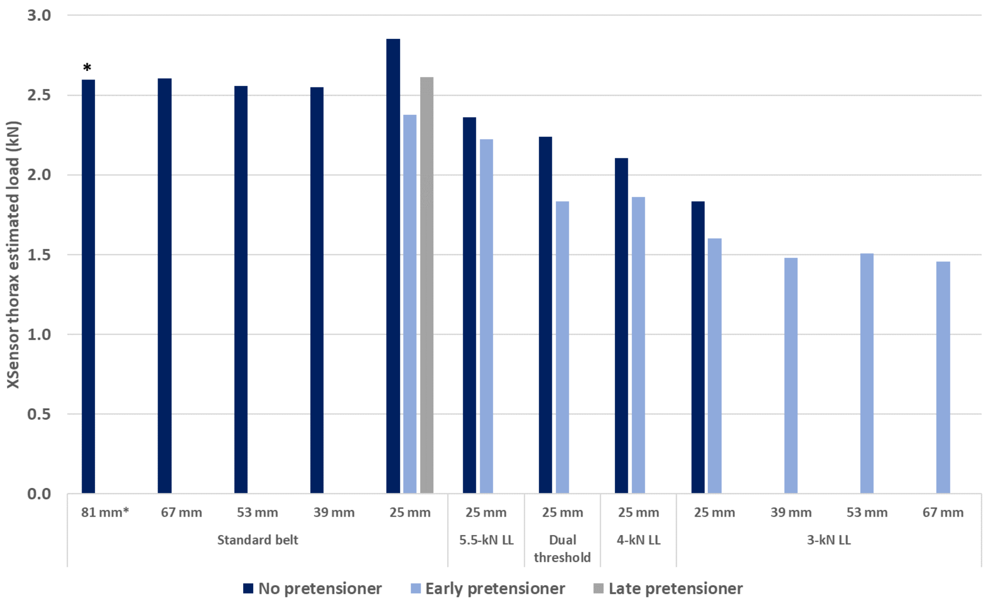

Fig. 13. Pressure mat thorax group estimated loads by belt position relative to chest potentiometer, pretensioner and load limiter characteristics. *One row of sensel data was lost for this condition, so values were interpolated from adjacent rows before calculating the cumulative load.

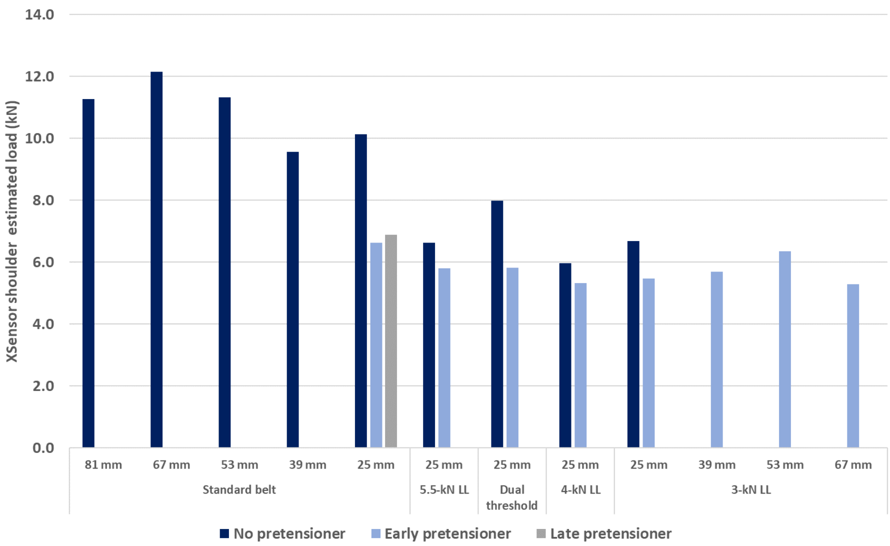

Fig. 14. Pressure mat shoulder group estimated loads by belt position relative to chest potentiometer, pretensioner and load limiter (LL) characteristics.

Fig. 15 shows the ratio of shoulder loads to thorax loads, which provides insight into the load distributions between the shoulder and thorax. Without belt technology, the shoulder group averages five times as much load as the thorax group. Belt technology (3 kN pretensioner and load limiter) decreases loads on the thorax and shoulder by 36% and 34%, respectively, at the 25 mm position, which decreases the ratio between the shoulder and thorax groups to 2.5.

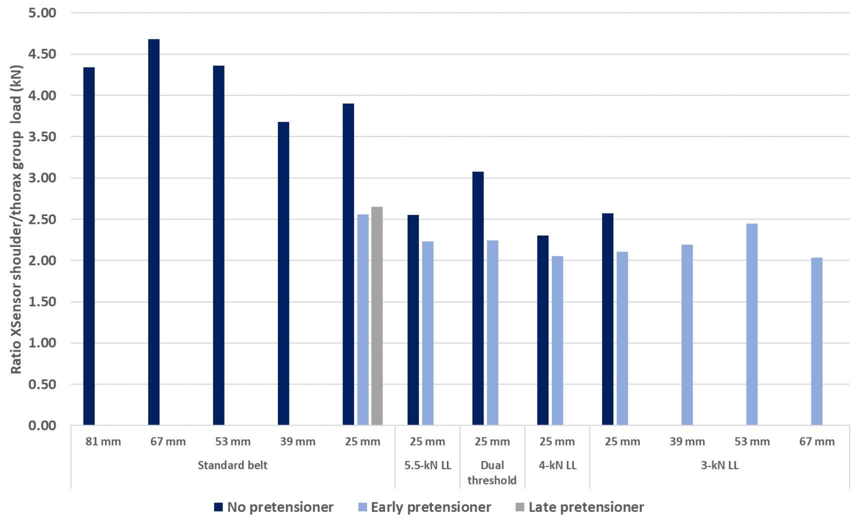

Fig. 15. Ratio of shoulder to thorax group estimated loads by belt position relative to chest potentiometer, pretensioner and load limiter characteristics.

IV. DISCUSSION

Thorax injuries are the dominant injuries for belted adults seated in the rear seat in frontal crashes. It is important for crash test programmes to use accurate, meaningful injury metrics to assess the relative risk of sustaining these injuries among vehicles in the fleet. This analysis provides insight on sternum deflection, thorax acceleration, electro-optical rib deflection, and pressure sensor mat estimated loads as thorax injury metrics for the Hybrid III 5th female dummy. It also quantifies their sensitivity to the beneficial belt technologies, force limiting and pretensioning, and the potential confounding factor of belt position.

For the Hybrid III family of dummies, the sternum deflection measured by a single rotary potentiometer attached to the sternum is the industry-accepted metric for assessing thorax injury risk in frontal crashes. In this study, sternum deflection on the Hybrid III 5th female reflected the benefit of force limiting, decreasing linearly 40% for a 3.5 kN decrease in shoulder belt tension with the belt placed in the same position. The benefits of force limiting in reducing real-world risk of thorax injury were observed by reference [18], who developed thoracic injury risk curves relating shoulder belt force to injury based on field cases. Reference [23] established a correlation between HIII 50th male sternum deflections and shoulder belt tension, showing that a 200 N increase in shoulder belt load resulted in a 1 mm increase in sternum deflection, but several other authors have observed test results related to sternum deflection measures that do not align with expectations based on belt tensions, similar tests with different belt positions or injury risk from field data [10,14,18,23], so it is important for consumer-information testing purposes to establish the pattern and magnitude of the sensitivity of the Hybrid III 5th female to this important safety countermeasure. For the HIII 5th female at a constant belt position, this study found that a 200 N increase in shoulder belt force resulted in a 1.1 mm increase in sternum deflection, which aligns closely with values reported by for the HIII 50th male [23]. In this study, sternum deflection also showed sensitivity to pretensioning, decreasing 5% for a pretensioner deployed at 14 ms compared to no pretensioning. These pretensioner results align with a study by reference [24], who also observed that that the HIII 5th showed sensitivity to pretensioning. The current study also showed that the sternum deflection metric is sensitive to the timing of pretensioning, which is an important restraint design variable. Deploying the pretensioner later in the current study, at 27 ms, increased the sternum deflection by 3%. Deploying the pretensioner later allows increased pelvis excursion which increases the longitudinal component of force imparted to the occupant by the shoulder belt. The primary aim of pretensioners is to couple the occupant to the vehicle early in the crash, which reduces accelerations and excursions, affecting loading on the thorax. Belt position has been observed as a confounding factor in sternum deflection results by several researchers [14,25-27]. In this study, increase in vertical belt position was strongly correlated with a reduction in sternum deflection. With the standard belt, moving the shoulder belt up on the thorax 56 mm decreased the sternum deflection by 15 mm, which is a 37% of the IARV change. For the standard belt and 3 kN force limiter/pretensioner belt, respectively, this represents a

2.7% and 2.3 % reduction in sternum deflection for every 5 mm of upward belt movement for the HIII 5th female. These results confirm the findings of previous researchers, but also provide quantitative data for understanding the magnitude of the relationship between belt location on the thorax and the effect on sternum deflection for the HIII 5th female. Other ATDs, like the THOR family of dummies, are in development to improve ATD thorax biofidelity and provide multi-axis and multi-point sensing for thorax deflection which offers an opportunity to reduce the sensitivity of these metrics to belt position or align the sensitivity with humans.

The dependence of chest deflection on belt position seen in this study underscores the conclusion from reference [9] that, "Reliance on chest deflection or chest acceleration to evaluate the performance of a restraint system could lead to inaccurate conclusions if the placement of the belt during loading is not taken into consideration." Reference [17] observed over 100 mm of variation in the pretest vertical belt position on the thorax in U.S. NCAP tests. Further variation is introduced with the dynamic movement of the belt due to pretensioning, belt-geometry-dictated load paths and the anatomical structures of the HIII 5th female [14]. To address the complications in locating the shoulder belt on the thorax at the time of maximum sternum deflection, the current study used the pressure sensor to locate the belt path. In this sled study, pretensioning did not affect belt placement and pressure mat belt path calculations at the onset of loading could be compared to pretest belt paths collected with a CMM for validation. Calculated pressure mat belt paths based on the centre of pressure on the pressure mat reliably replicated the belt paths recorded pretest, reporting a 27 mm vertical belt path distance from the sternum potentiometer compared to 25 mm recorded pretest. The dynamic location of the belt coupled with quantitative data on the effect of belt positioning on sternum deflection provides consumer-information testing programmes with additional information to interpret and compare the sternum deflection results between vehicles. This study found a consistent relationship between the inferior-superior belt position and percent change in sternum deflection while varying load-limiting, but additional factors like belt anchor locations, buckle and seat designs could influence this relationship.

Thorax spine acceleration showed sensitivity to force limiting and pretensioning that aligned with sternum deflection, but instead of increasing with later pretensioner timing, thorax acceleration decreased. Thorax acceleration also showed little sensitivity to belt positioning, only changing 3% of IARV for 56 mm of change in belt position. The direction of sensitivity, however, was also in contrast with the sternum deflection and this is due to the change in how the rib cage is loaded with different belt paths. As seen in Fig. 10, lower belt positions loaded the ribs medially, which deflects the ribs. Higher belt positions loaded the curved aspect of the rib, translating the force on the ribs to the spine and increasing acceleration in the x-direction and reducing the torso rotations about the lateral axis. Thorax spine acceleration "sums the effects of force inputs from the ribcage, shoulder and arms, abdomen, neck and lumbar spine", which does not necessarily represent the rib cage compression injuries that cause rib fracture and organ injury [8]. According to reference [28], "Measurements of direct load applications such as force and chest deflection are authoritative indicators of dummy load paths. Global measures such as acceleration clips provide only a snapshot in time and do not adequately describe the severity or duration of the loading event."

The electro-optical rib deflection system was included to explore opportunities for sternum deflection measures that could be less sensitive to belt path. In this study, the electro-optical rib sensor resultant deflections showed sensitivity to force limiting and pretensioning when the belt was held constant like sternum deflection, but also showed sensitivity to belt position. Though the rib reporting maximum deflection moved up with increasing belt position, the peak deflection reported still decreased the same amount as the sternum deflection relative to lower positions. In contrast, previous studies by reference [25] using the HIII 50th male found that when peak sternum deflection decreased as the belt moved up on the thorax, the peak resultant deflection did not decrease. This discrepancy between electro-optical rib deflection results for the HIII 50th and 5th could be the result of dummy anthropometry or sensor locations. Reference [28] studied the same electro-optical rib deflection system on the HIII 5th female and found that the rib sensors captured both lateral and vertical asymmetrical loading with change in belt position, but reported that ratios between electro-optical rib deflections and sternum potentiometer deflection changed with belt position. The current study found a consistent maximum resultant rib deflection to sternum deflection ratio of 1.1 across all standard belt positions, indicating that the maximum resultant electro-optical rib deflection shows a sensitivity to belt placement similar to sternum deflection. The electro-optical rib deflection sensor provided information on load distributions in this study, indicating that the right ribs experienced high deflection and that the lower right ribs are the most sensitive to changes in belt position. Reference [27] also noted that this same electro-optical rib deflection system is good for understanding asymmetry, but expressed concern that it lacks information about biomechanical value. For example, the peak resultant deflection reported by each rib decreased and the maximum resultant deflection reported by any rib decreased as the belt moved higher on the torso in this study, but we do not have biomechanical data to understand if this decrease provides meaningful benefit for real-world occupants or is an artifact of dummy construction. Lower rib sensors also experienced interference from the sternum potentiometer arm, which resulted in data loss. The electro-optical rib deflection system provides both A-P and L-M deflections, which could be valuable in understanding the sensitivity of the sternum resultant deflections to belt position. One possible contributor to the sternum deflection sensitivity could be a change in the axis of deflection, where A-P deflections decrease and L-M deflections increase (though not enough to keep the resultant from decreasing). However, this was not observed for the HIII 5th female dummy in these conditions. Both A-P and L-M deflections decreased in magnitude in these tests with higher belt positions. Other researchers have evaluated both A-P and L-M deflections in understanding ATD response to restraint variables [29], but this relationship does not seem to account for the sensitivity to belt position for the HIII 5th with the sensor locations used in this test series. Other metrics like increased thorax acceleration and decreased y-axis torso rotation account for some of the difference in sternum deflections at higher belt position, but other metrics that were not measured like z-axis torso rotation may also be contributors.

The pressure sensor loads lack biomechanical data for injury correlation, so individual group loads were compared with sternum deflection responses as a starting point to understand their relevance. When belt position was held constant, the thorax region loads strongly correlated with sternum deflection for changes in force limiting and pretensioning. The shoulder group loads, however, did not have a strong correlation with sternum deflection. Since sternum deflection is meant to reflect only loads applied directly to the thorax, these results align with expectations and indicate that the pressure mat is providing relevant information on the magnitude and distribution of loads between the shoulder and torso. Thorax group loads and sternum deflection diverge, however, in their sensitivity to belt position. Loads reported for the thorax group do not show the linear correlation with belt position seen with sternum deflection and thus offer potential to measure injury-causing loads on the thorax irrespective of belt position. The thorax group loads did have elevated values at the lowest belt position. This result may be due to dummy design or may represent a real increase in load due to the belt path on the thorax and belt interactions with dummy ribs. Like sternum deflection, deflections from the electro-optical sensor showed a downward trend with belt position which does not align with loads on the thoracic region of the pressure sensor. However, analysis of the local pressures in the right rib 6 region, where the largest differences were seen in the electro-optical sensor deflections between the extreme positions (25 mm and 81 mm), shows regions of higher pressure for the 25 mm position vs the 81 mm. This result supports the elevated increase in rib 6 deflections relative to other ribs observed for lower belt positions. The pressure sensor also provided ratios for shoulder to thorax loading, indicating that the shoulder carries 5 times higher loads than the thorax with the standard belt. The addition of technology reduces both shoulder and thorax group loads by approximately 35%, reducing shoulder to thorax ratios to 2.5 for all combinations of technology. Loads on the thorax calculated using the region of the pressure mat covering the ribs generally align with upper belt tension early in the test when considering component forces and rotation of the dummy. Later in the test, other factors like lower shoulder belt tension, z-axis torso rotation and pelvis excursions affect the loading to the thorax. Further research is ongoing to analyze additional regions of the pressure sensor and fully understand the results provided by the sensor.

The results of this study are limited by the lack of variance in the testing environment and test conditions. Tests were conducted on an acceleration sled in a simulated environment that may eliminate the influence of dynamic factors in vehicle crash tests. The simulated environment was limited to one seat style and one set of lower anchor positions, which could affect the influence of parameters on outcomes. The seat used was reinforced to prevent fatigue and was checked after each test for wear, but the same seat was used for all tests and unobservable changes in the seat foam or cover could have affected the results. No dynamic testing was conducted without the XSensor to verify that it does not influence the sensitivity of sternum deflection to belt position. However, calibration testing was conducted both with and without the pressure sensor and the force-deflection results were well aligned.

V. CONCLUSION

Sternum deflection, thorax acceleration, electro-optical rib deflections and pressure mat thorax group loads all showed sensitivity to both force limiting and pretensioning. Sternum deflection and electro-optical rib deflections, however, also showed a strong linear correlation with belt position, and this could have implications for crash test programmes when comparing the relative protection of restraint systems. Thorax acceleration did not show sensitivity to belt position but is also not a reliable predictor of thorax compression injury. The relationship between electro-optical rib deflections and belt position indicates that the sensitivity of the sternum potentiometer to belt position is not only due to loading farther from the sensor, but also possibly due to the shape and design of the HIII 5th female thorax relative to the location of load. The pressure sensor provided accurate dynamic belt positions and coupled with quantitative data on the effect of belt position on sternum deflection for the HIII 5th female provides consumer-testing organisations with additional information to aid in interpreting vehicle crash test sternum deflection results. The pressure mat thorax group loads had strong correlations with sternum deflection when the belt position was constant, but showed little sensitivity to belt position indicating the sensor provides relevant information on load magnitude and distribution irrespective of belt position.

VI. ACKNOWLEDGEMENTS

The authors greatly appreciate the generous support for this research and would like to thank Autoliv for the donation of seat belts, XSensor for the loan of sensor equipment, and Honda and General Motors for the loan of RibEye systems. We would also like to thank Boxboro systems for equipment support.

VII. REFERENCES

[1] Insurance Institute for Highway Safety. Major change in frontal crashworthiness evaluations. *Status Report*, 2006. 41(3): p. 1-7

[2] Kahane, C.J. Correlation of NCAP Perfromance with Fatality Risk in Actual Head-on Collicions. NHTSA Technical Report. . 1994.

[3] Kahane, C.J. Effectiveness of pretensioner and load limiters for enhancing fatility reduction by seat belts. 2013, National Highway Traffic Safety Administration: Washington, DC.

[4] Barry, K. Making back seats safer: When it comes to safety advances, the back seat hasn't kept pace with the front—But that could be about to change, in *Consumer Reports*. 2020.

[5] Durbin, D.R., Jermakian, J.S., et al. Rear seat safety: Variation in protection by occupant, crash and vehicle characteristics. *Accident Analysis & Prevention*, 2015. 80: p. 185-192

[6] Jermakian, J., Edwards, M., Fein, S., and Maltese, M.R. Factors contributing to serious and fatal injuries in belted rear seat occupants in frontal crashes. *Traffic Injury Prevention*, 2019. 20(sup1): p. S84-S91

[7] Kuppa, S., Saunders, J., and Fessahaie, O. Rear seat occupant protection in frontal crashes. *Proceedings of 19th International Technical Conference on the Enhanced Safety of Vehicles (ESV)*, 2005. Washington, DC

[8] Horsch, J.D., Melvin, J.W., Viano, D.C., and Mertz, H.J. Thoracic injury assessment of belt restraint systems based on Hybrid III chest compression. *SAE Transactions*, 1991. 100: p. 1875-1898

[9] Tylko, S. and Bussières, A. Responses of the Hybrid III 5th female and 10-year-old ATD seated in the rear seats of passenger vehicles in frontal crash tests. *Proceedings of 2012 IRCOBI Conference*, 2012. Dublin, Ireland

[10] Brumbelow, M.L. Can front crash rating programs using Hybrid III predict real world thoracic injuries? *Proceedings of 2020 IRCOBI Conference*, 2020.

[11] Hu, J., Reed, M.P., et al. Optimizing Seat Belt and Airbag Designs for Rear Seat Occupant Protection in Frontal Crashes. *Proceedings of 61st Stapp Car Crash Conference*, 2017.

[12] Brumbelow, M.L., Jermakian, J.S., Arbelaez, R.A. . THOR analysis. *Predicting real-world thoracic injury using THOR and Hybrid III crash tests. Proceedings of IRCOBI Conference, in press.*, 2022

[13] Bose, D., Crandall, J., Forman, J., Longhitano, D., and Arregui-Dalmases, C. Epidemiology of injuries sustained by rear-seat passengers in frontal motor vehicle crashes. *Journal of Transport & Health*, 2017. 4: p. 132-139

[14] Tylko, S., Higuchi, K., Lawrence, S.S., Bussières, A., and Fiore, J.M. A comparison of Hybrid III 5th female dummy chest responses in controlled sled trials. *SAE Transactions*, 2006: p. 283-290

[15] Yamasaki, T. and Uesaka, K. Rear occupant protection JNCAP test—Test results and findings. *Proceedings of 22nd International Technical Conference on the Enhanced Safety of Vehicles (ESV)*, 2011. Washington, DC

[16] Beck, B., Brown, J., and Bilston, L.E. Assessment of vehicle and restraint design changes for mitigating rear seat occupant injuries. *Traffic injury prevention*, 2014. 15(7): p. 711-719

[17] Haight, S., Samaha, R.R., and Biss, D. Analysis of seat belt positioning in recent NCAP crash tests. *SAE International Journal of Transportation Safety*, 2013. 1(1): p. 16-24

[18] Foret-Bruno, J.Y., Trosseille, X., et al. Thoracic injury risk in frontal car crashes with occupant restrained with belt load limiter. *Proceedings of 42nd Annual Stapp Car Crash Conference*, 1998. Tempe Arizona,

[19] Forman, J., Michaelson, J., Kent, R., Kuppa, S., and Bostrom, O. Occupant restraint in the rear seat: ATD responses to standard and pre-tensioning, force-limiting belt restraints. *Annals of Advances in Automotive Medicine*, 2008. 52: p. 141-154

[20] Society of Automotive Engineers. Instrumentation for impact test – Part 1 – Electronic instrumentation, in *Surface Vehicle Recommended Practice (J211)*. 1995, SAE International: Warenton, PA, USA.

[21] Insurance Institute for Highway Safety. Dummy seating procedure for rear outboard positions (Version II Draft). 2020, October: Ruckersville, VA.

[22] Mertz, H.J., Irwin, A.L., and Prasad, P. Biomechanical and scaling basis for frontal and side impact injury assessment reference values. *Stapp car crash journal*, 2016. 60: p. 625

[23] Mertz, H.J., Horsch, J.D., Horn, G., and Lowne, R.W. Hybrid III sternal deflection associated with thoracic injury severities of occupants restrained with force-limiting shoulder belts. *SAE Transactions*, 1991: p. 1108-1122

[24] Bohman, K. and Fredriksson, R. Pretensioner loading to rear-seat occupants during static and dynamic testing. *Traffic Injury Prevention*, 2014. 15(sup1): p. S111-S118

[25] Eggers, A. and Adolph, T. Evaluation of the thoracic deflection measurement system 'RibEye' in the Hybrid III 50% in frontal sled tests. *Proceedings of 22nd International Technical Conference on the Enhanced Safety of Vehicles (ESV)*, 2011. Washington, DC

[26] Eggers, A., Eickhoff, B., Dobberstein, J., Zellmer, H., and Adolph, T. Effects of variations in belt geometry, double pretensioning and adaptive load limiting on advanced chest measurements of THOR and Hybrid III. *Proceedings of 2014 IRCOBI Conference*, 2014. Berlin, Germany

[27] Digges, K., Dalmotas, D., Prasad, P., and Mueller, B. The need to control belt routing for Silver NCAP ratings. *Proceedings of 25th International Technical Conference on the Enhanced Safety of Vehicles (ESV)*, 2017. Detroit, MI

[28] Tylko, S., Charlebois, D., and Bussières, A. Comparison of kinematic and thoracic response of the 5th percentile Hybrid III in 40, 48 and 56 km/h rigid barrier tests. *Proceedings of 20th International Technical Conference on the Enhanced Safety of Vehicles (ESV)*, 2007. Lyon, France

[29] Kent, R., Lessley, D., Shaw, G., and Crandall, J. The utility of Hybrid III and THOR chest deflection for discriminating between standard and force-limiting belt systems. *Stapp car crash journal*, 2003. 47: p. 267

VIII. APPENDIX

TABLE A-I
TEST CONDITIONS AND RESULT METRICS

	Force limiter	Pretensioner	Static belt position	Shoulder belt load	Shoulder belt load peak time	Sternum deflection	Sternum deflection peak time	Thorax resultant acceleration (3-ms clip)	Thorax resultant acceleration peak time		Thorax rotation	Thorax rotation peak time	Test ID
									T1	T2			
			mm	kN	ms	mm	ms	g	ms	ms	Deg	ms	
Static/dynamic belt position	None	None	25	6.48	106.0	−48.33	115.9	39.05	76.7	79.7	−31.98	120.8	SF20005
	None	None	39	6.24	107.0	−43.54	113.2	39.48	78.6	83.6	−28.21	118.6	SF20006
	None	None	53	6.34	106.6	−40.46	112.6	41.30	80.0	83.0	−27.94	119.3	SF20007
	None	None	67	6.31	105.9	−38.36	111.1	41.97	79.4	82.4	−25.97	117	SF20008
	None	None	81	6.53	105.1	−33.55	109.1	41.03	78.3	81.3	−26.54	115.7	SF20009
Pretensioning	None	Early	25	6.18	109.4	−45.67	112.1	34.02	94.9	99.6	−23.20	121.6	SF20010b
	None	Late	25	6.39	104.5	−49.55	112	33.45	98.7	101.7	−25.12	121.4	SF20011
Force limiting	3	None	25	3.06	133.0	−29.44	104.2	26.91	78.1	81.1	−81.81	157.4	SF20014b
	4	None	25	4.48	71.9	−39.40	117.3	33.69	70.7	73.7	−50.70	133.1	SF20013
	5.5	None	25	5.46	83.6	−44.67	116	40.15	77.9	80.9	−34.42	124.4	SF20012
	Dual	None	25	5.03	121.9	−41.16	125.3	31.93	77.7	80.7	−55.14	134.6	SF20015
Combined pretensioning and force limiting	3	Early	25	2.88	56.2	−27.89	113.8	22.90	98.7	101.7	−75.55	180.9	SF20016
	4	Early	25	3.95	118.0	−36.42	114.1	26.13	97.8	100.8	−41.08	143.3	SF20017
	5.5	Early	25	5.51	90.9	−44.78	114.2	29.81	98.3	101.3	−29.31	127.4	SF20018
	Dual	Early	25	4.00	110.6	−34.77	112.2	26.81	98.7	104.1	−47.12	144.7	SF20019
Combined pretensioning, force limiting and belt position	3	Early	39	2.88	134.6	−26.19	112.2	23.49	98.4	101.4	−71.78	176.3	SF20020
	3	Early	53	2.81	121.5	−23.90	113.8	23.90	99.0	103.7	−65.31	169.5	SF20021
	3	Early	67	3.02	64.9	−22.46	114.4	24.71	101.4	105.4	−60.59	161.4	SF20022

TABLE A-II
TEST CONDITIONS AND RESULT METRICS, CONTINUED

	Force limiter	Pretensioner	Static belt position	Pressure Sensor thorax load	Pressure Sensor shoulder load	Pressure Sensor combined	Test ID
			mm	kN	kN	kN	
Static/dynamic belt position	None	None	25	2.85	10.13	12.98	SF20005
	None	None	39	2.55	9.56	12.11	SF20006
	None	None	53	2.56	11.32	13.88	SF20007
	None	None	67	2.60	12.16	14.76	SF20008
	None	None	81	2.60*	11.27	13.87*	SF20009
Pretensioning	None	Early	25	2.38	6.25	6.64	SF20010b
	None	Late	25	2.61	6.46	6.89	SF20011
Force limiting	3	None	25	1.83	6.55	6.68	SF20014b
	4	None	25	2.11	5.98	8.09	SF20013
	5.5	None	25	2.36	6.63	8.99	SF20012
	Dual	None	25	2.24	7.99	10.23	SF20015
Combined pretensioning and force limiting	3	Early	25	1.60	5.47	7.07	SF20016
	4	Early	25	1.86	5.33	7.19	SF20017
	5.5	Early	25	2.22	5.80	8.02	SF20018
	Dual	Early	25	1.83	5.82	7.65	SF20019
Combined pretensioning, force limiting and belt position	3	Early	39	1.48	5.70	7.18	SF20020
	3	Early	53	1.51	6.36	7.87	SF20021
	3	Early	67	1.46	5.29	6.75	SF20022

*One row of sensel data was lost for this condition, so values were interpolated from adjacent rows before calculating the cumulative load.

TABLE A-III
TEST CONDITIONS AND RESULT METRICS, CONTINUED

	Force limiter	Pretensioner	Static belt position	RibEye Resultant Left Rib 1	RibEye Resultant Left Rib 2	RibEye Resultant Left Rib 3	RibEye Resultant Left Rib 4	RibEye Resultant Left Rib 5	RibEye Resultant Left Rib 6	RibEye Resultant Right Rib 1	RibEye Resultant Right Rib 2	RibEye Resultant Right Rib 3	RibEye Resultant Right Rib 4	RibEye Resultant Right Rib 5	RibEye Resultant Right Rib 6	RibEye maximum	Rib reporting maximum	Test ID
			mm	mm	mm	mm	mm	mm	mm	mm	mm	mm	mm	mm	mm	mm		
Static/ dynamic belt position	None	None	25	32	32	32	X	X	X	47	49	49	52	X	X	52	Rib 4	SF20005
	None	None	39	29	29	28	27	X	X	44	45	46	47	48	49	49	Rib 6	SF20006
	None	None	53	27	27	26	24	X	X	42	43	43	43	44	44	44	Rib 6	SF20007
	None	None	67	25	24	23	22	X	X	40	41	41	41	41	41	41	Rib 2	SF20008
	None	None	81	22	21	20	18	17	X	37	37	36	36	35	34	37	Rib 2	SF20009
Pretensioning	None	Early	25	32	32	31	30	X	X	45	46	46	47	49	50	50	Rib 6	SF20010b
	None	Late	25	33	34	33	X	X	X	46	48	49	51	X	X	51	Rib 4	SF20011
Force limiting	3	None	25	23	22	22	21	20	19	28	29	29	29	30	31	31	Rib 6	SF20014b
	4	None	25	28	28	29	28	27	X	39	40	40	42	43	44	44	Rib 6	SF20013
	5.5	None	25	30	31	31	30	29	X	43	45	45	47	49	X	49	Rib 5	SF20012
	Dual	None	25	30	30	30	29	28	X	40	42	41	43	44	45	45	Rib 6	SF20015
Combined pretensioning and force limiting	3	Early	25	22	22	22	20	19	19	26	27	26	26	27	28	28	Rib 6	SF20016
	4	Early	25	27	27	27	26	25	X	35	36	36	36	38	39	39	Rib 6	SF20017
	5.5	Early	25	X	X	X	X	X	X	X	X	X	X	X	X	X	X	SF20018
	Dual	Early	25	26	26	26	25	23	X	35	35	34	35	35	36	36	Rib 6	SF20019
Combined pretensioning, force limiting and belt position	3	Early	39	21	20	20	19	17	17	24	25	24	24	25	X	25	Rib 2	SF20020
	3	Early	53	19	18	17	16	15	X	23	23	23	22	22	X	23	Rib 2	SF20021
	3	Early	67	17	17	16	14	13	X	22	22	21	20	20	X	22	Rib 2	SF20022

TABLE A-IV
TEST CONDITIONS AND RESULT METRICS, CONTINUED – RIBEYE SENSOR DEFLECTIONS

Test_ID	Rib 1				Rib 2				Rib3				Rib 4				Rib 5				Rib 6			
	Left		Right		Left		Right		Left		Right		Left		Right		Left		Right		Left		Right	
	X	Y	X	Y	X	Y	X	Y	X	Y	X	Y	X	Y	X	Y	X	Y	X	Y	X	Y	X	Y
	mm	mm	mm	mm	mm	mm	mm	mm	mm	mm	mm	mm	mm	mm	mm	mm	mm	mm	mm	mm	mm	mm	mm	mm
SF20005	-31	6	-45	15	-31	7	-46	16	-31	10	-48	14	X	X	-50	14	X	X	X	X	X	X	X	X
SF20006	-29	5	-42	14	-28	6	-43	14	-27	9	-44	12	-26	9	-45	12	X	X	-46	14	X	X	-48	14
SF20007	-27	4	-40	12	-26	5	-41	12	-25	7	-42	10	-23	8	-42	11	X	X	-42	12	X	X	-43	12
SF20008	-25	3	-39	11	-24	4	-40	10	-23	6	-40	8	-21	6	-40	9	X	X	-40	10	X	X	-40	10
SF20009	-22	2	-36	9	-21	2	-36	8	-20	4	-36	6	-18	4	-35	6	-17	3	-34	7	X	X	-33	8
SF20010b	-32	6	-42	15	-31	7	-43	16	-30	10	-44	14	-29	10	-45	14	X	X	-46	15	X	X	-48	15
SF20011	-33	5	-44	14	-33	6	-46	15	-32	9	-47	13	X	X	-49	14	X	X	X	X	X	X	X	X
SF20014b	-22	7	-24	15	-21	8	-26	14	-20	9	-26	13	-19	9	-26	13	-19	8	-26	14	-18	9	-28	14
SF20013	-27	8	-36	16	-27	9	-37	17	-26	11	-38	15	-26	11	-39	16	-25	10	-39	17	X	X	-41	17
SF20012	-30	6	-40	15	-30	8	-42	16	-29	10	-43	14	-28	11	-45	15	-28	9	-46	17	X	X	X	X
SF20015	-29	8	-37	17	-29	9	-38	18	-28	12	-39	16	-27	11	-40	17	-26	10	-40	18	X	X	-42	18
SF20016	-21	6	-23	13	-21	7	-23	14	-20	9	-23	12	-19	9	-23	13	-18	7	-24	13	-18	9	-24	14
SF20017	-26	7	-32	16	-26	8	-33	16	-25	10	-33	14	-24	10	-33	15	-23	9	-34	16	X	X	-36	16
SF20018	X	X	X	X	X	X	X	X	X	X	X	X	X	X	X	X	X	X	X	X	X	X	X	X
SF20019	-25	8	-31	16	-25	9	-31	16	-24	10	-31	14	-23	10	-32	15	-22	9	-32	16	X	X	-33	16
SF20020	-20	6	-21	12	-20	6	-22	12	-19	8	-22	11	-18	7	-22	11	-17	7	-22	12	-16	8	X	X
SF20021	-18	4	-20	11	-18	5	-21	10	-17	6	-21	9	-16	6	-21	10	-15	5	-20	10	X	X	X	X
SF20022	-17	2	-20	8	-17	3	-21	8	-16	3	-21	6	-14	3	-20	6	-13	2	-19	7	X	X	X	X

TABLE A-V
SENSOR MODEL NUMBERS AND FILTERING

Sensor	Model #	Filter
Shoulder belt load	Messring 5BC-D16-21A	SAE CFC-60
Sternum potentiometer	SERVO 14CB1-3178 1K +/- 10%	SAE CFC-600
Spine accelerometer	Endevco 7264A-2000	SAE CFC-180
Spine angular rate	DTS ARS Pro – 18k	SAE CFC-180
XSensor	HX210:30.40.05-15M HSS [S0001]	XSensor Zero pressure filter and Anti-speckle filter
RibEye	RibEye Hybrid III ATD 5th female, 2-axis	SAE CFC-600

TABLE A-VI
H-POINT, HEAD CG, ANCHOR LOCATION AND PELVIS ANGLE

	H-point			Head CG			Upper anchor			Pelvis angle
	X	Y	Z	X	Y	Z	X	Y	Z	
Test ID	mm	mm	mm	mm	mm	mm	mm	mm	mm	Deg
SF20005	1178	831	386	1319	500	952	1694	235	984	20.0
SF20006	1178	833	391	1324	502	958	1692	275	983	20.8
SF20007	1176	833	389	1324	502	954	1692	279	982	20.7
SF20008	1174	834	388	1326	508	956	1692	309	983	20.3
SF20009	1177	825	383	1325	502	955	1696	313	984	20.9
SF20010b	1177	828	390	1323	497	956	1693	235	984	20.9
SF20011	1177	822	388	1319	499	960	1692	237	986	20.1
SF20014b	1176	832	392	1333	498	955	1693	237	982	20.9
SF20013	1177	828	386	1326	499	955	1695	233	983	20.7
SF20012	1176	832	395	1323	500	960	1696	229	984	20.5
SF20015	1176	834	393	1325	504	959	1694	235	983	20.3
SF20016	1176	827	388	1322	499	957	1692	236	983	20.8
SF20017	1173	826	393	1322	496	957	1693	234	986	20.9
SF20018	1178	836	396	1324	501	959	1694	233	985	20.9
SF20019	1174	820	388	1327	499	958	1691	235	982	20.8
SF20020	1178	824	395	1323	494	961	1691	236	982	20.5
SF20021	1175	828	395	1324	499	961	1690	279	983	20.6
SF20022	1177	821	389	1327	503	961	1690	316	981	20.0